SAND2013-8985C

Measuring Effective Mass of a Circuit Board

Randall L. Mayes
Experimental Mechanics, NDE and Model Validation Department
Sandia National Laboratories*
P.O. Box 5800 - MS0557
Albuquerque, NM, 87185
rlmayes@sandia.gov

Daniel W. Linehan
ATA Engineering
11995 El Camino Real, Suite 200
San Diego, CA, 92130dan.linehan@ata-e.com

Nomenclature

DoF	degree of freedom
FRF	frequency response function
SDoF	single degree of freedom
f	force
mm_k	modal mass for mode k
m_{TA}	mass of the test article
M_B	mass of the fixture or base
pmpf(k)	pseudo-modal participation factor for mode *k*
P_k	modal participation factor in one direction for mode *k*
$\ddot{x}$	acceleration in one direction
q	generalized coordinate
$\mathbf{L}$	reduction matrix applying the constraint to equations of motion
Φ	rigid body mode shape vector with ones in the direction of interest
Ψ	mass normalized real mode shape matrix
Γ	eigenvectors resulting from constraint equations
B	subscript for the fixture or base
k	subscript for mode number
TA	subscript for the test article

*Sandia National Laboratories is a multi-program laboratory operated by Sandia Corporation, a wholly owned subsidiary of Lockheed Martin Corporation, for the U.S. Department of Energy National Nuclear Security Administration under Contract DE-AC04-94AL85000.

1) Abstract

Effective mass is a system property of a base mounted structural mode of vibration in a specific system axis. Effective mass is usually calculated with the finite element model. A method of deriving effective mass from dynamic measurements on the hardware was presented previously. The method is applied to a circuit board mounted on a fixture for the out of plane axis. The uncertainty of the method is evaluated using a nylon plate truth model of about the same dimensions and weight as the circuit board. The method measures frequency response functions on the fixture supporting the circuit board. Modes are extracted, and the mode shapes are processed to estimate the effective mass of each fixed base mode. These results will ultimately be used to support energy based failure analysis on the circuit board.

Keywords – Effective Mass; Modal Participation Factor; Experimental

2) Motivation and Application

Sandia National Laboratories has proposed a fatigue-damage metric based on the cumulative dissipated energy in a linear superposition of singe-degree-of-freedom (SDoF) modal models as part of a framework for predicting failure of components subjected to random vibration loading. Savoie and Babuska[1] have applied this to a circuit board and presented the results at this conference. In order to utilize the proposed framework, the effective mass is required for the SDoF modal models. Usually this is obtained from finite element model (FEM) calculations, but in many cases, a FEM may not exist. In addition, the FEM may not be verified. It is desirable to have an experimental method to calculate the fixed base natural frequency and the effective mass of each of the lower modes of the component. If the test article is available, it can be mounted on a fixture and a free modal test performed to extract parameters that can be utilized to calculate effective mass as shown by Mayes et al.[2]. In their work they showed that effective mass could be measured for the first 10 modes in one direction within about four percent of the test article mass. Their work addressed a test article with a mass of 72 kg for modes from about 35 to 1350 Hz. Here we wish to extract the effective mass for Savoie and Babuska's circuit board with a mass of 42.41 g and modal frequencies from 130 to 2300 Hz.

In order to establish the uncertainty of the method for this class of test article, the effective mass experiment and calculation is applied to a "truth" structure which is a uniform nylon plate with the same length and width and almost the same weight as the circuit board. Both will be attached to an aluminum plate fixture with two posts to which the circuit board (or truth structure) are attached. One can see the circuit board as well as the truth structure attached to the fixture in Figure 1. Since the truth test article is relatively simple, a FEM of the truth structure was generated to calculate effective mass. The "truth" effective mass in the out of plane direction is calculated, and the test effective mass will be compared to that to quantify uncertainty of the effective mass from the test approach. Finally, the test effective mass will be extracted for the real circuit board and the uncertainty is assumed to be the same as derived from the truth test.

Figure 1 - Circuit Board and Fixture (Left), Truth Plate and Fixture (Right)

3) Effective Mass Concept and History

The effective mass offers a physical interpretation of a physical system with multiple modes of vibration being excited dynamically from a base, similar to testing that occurs for many systems. The concept was proposed in the early 70's by Bamford[3] with others. For a base excited system, it is represented as attached to a massless base, which will be excited in

only one direction with acceleration, $\ddot{x}$, with each mode represented by a single degree of freedom oscillator as shown in Figure 2. The mass of each oscillator is valued so that it is the effective mass of the respective mode of vibration. The springs are scaled so that the mass vibrates at the appropriate modal frequency. In general, only the modes that have the significant effective masses are required to represent the response up to some desired frequency. In the figure we show four such modes. The other modes are truncated. The effective mass of all the truncated modes is added directly to the base as a residual mass. When the base is accelerated with some vibration specification, the various effective mass oscillators will impose the correct reaction force on the base in the direction of excitation. As can be seen from this illustration, effective mass is based on a system that can be represented as having a base input. It depends also on the assumption that the base is rigid.

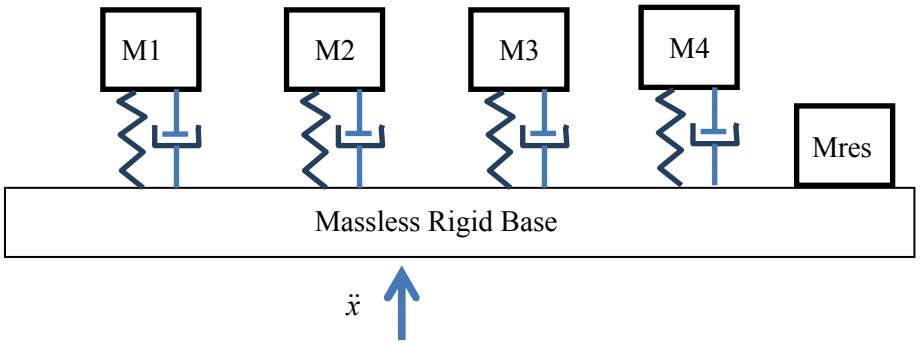

Figure 2 - Physical Picture of Effective Mass Concept

Effective mass is related to modal participation factor, P_k. The derivations of modal participation factor and effective mass can be found in the FEMA 451B Topic 4 Notes [10]. A major difference between effective mass and modal participation factor is that modal participation factor is different depending on the scaling of the modal mass, mm_k, whereas effective mass is a single defined value. In a fixed base eigenvalue problem of an analytical model of the system, the modal participation factor multiplied by $-\ddot{x}$ provides the modal force that will excite a particular mode for the rigid base acceleration, $\ddot{x}$. The effective mass, which provides the actual base reaction force associated with a particular mode, resolves any question about mode shape scaling and is calculated as

$$m_{eff,k} = P_k^2 mm_k . \tag{1}$$

If Ψ_{fixed}^{k} is the fixed base mode shape vector for mode k and $\mathbf{M}$ is the mass matrix of the test article, the modal participation factor can be calculated from the rigid body mode shape vector, Φ, of the system released and translating in the direction of acceleration of the base as

$$P_k = \overline{\Phi}^T \mathbf{M} \overline{\Psi}_{fixed}^{k} / mm_k \tag{2}$$

where the rigid body shape values of vector Φ in the direction of acceleration are equal to one and in orthogonal directions are equal to zero. The modal participation factor and effective mass are related to direction. If vector Φ represents the rigid body mode shape in the y direction, as opposed to the x direction as shown in the figure, a different modal participation factor (and effective mass) will be calculated for mode k.

As can be seen, this standard approach requires a finite element model. If the finite element model is in error, the modal participation factor and effective mass will be in error.

4) Effective Mass Measurement Approach

The method of Mayes[2] will be utilized for this application. The effective mass of each mode is desired for the out of plane (vertical) direction for the nylon plate and the circuit board shown in Figure 1. The steps to obtain the effective mass are:

1. Perform a freely supported modal test on the fixture to determine its elastic shapes that might be in the frequency band of interest. The fixture must be instrumented so that all the rigid body shapes and any elastic shapes extracted are independent (so the test mode shape matrix may be inverted).

2. Perform a freely supported modal test on the test article mounted to the fixture. The fixture must be instrumented but it is not required that the test article be instrumented.
3. Constrain the test article and fixture so that all elastic modes of the fixture and rigid body rotation modes and rigid body lateral modes are constrained to zero. Only one rigid body mode in the vertical direction and elastic modes of the attached test article remain.
4. Calculate the pseudo modal participation factors from the partially constrained modal results of step 3, which requires the mode shape of the fixture, the mass of the fixture and the mass of the test article.
5. Constrain the final rigid body mode to zero displacement using data from step 3 and capture the **L** matrix and resulting **Γ** modal vectors.
6. Finally calculate the fixed base modal participation factor estimates using pseudo modal participation factors from step 4 and the **L** and **Γ** matrices from step 5. Then eqn (1) can be utilized to calculate the effective mass for each mode.

This work is made possible by the recent theory[4-7] that can be applied to mode shapes gathered from an unconstrained modal test to constrain the modal degrees of freedom of the test fixture to which the test article is connected. The **L** matrix is the matrix that applies the constraints to an unconstrained system in the primal formulation of dynamic substructuring (see De Klerk, Rixen and Voormeeren's, framework for all substructuring methods[8]). The **Γ** matrix is the matrix of eigenvectors resulting from the eigenvalue problem solution on the constrained system.

5) Abbreviated Effective Mass Measurement Theory

The derivation of the theory for extracting experimental effective mass was published[2] and will not be repeated here. The pertinent final equations are given below. The required measurements are the modal mass of each mode, the mode shapes measured on the fixture, the mass of the fixture and the mass of the test article. The mode shapes must include the rigid body modes and any elastic modes of the fixture that may influence results in the frequency band of interest. No measurement of the mode shape on the test article is required, but it may provide valuable insight. The mode shapes are constrained so that:

1. elastic modes of the fixture have been constrained; and
2. all rigid body modes are constrained except the one in the direction for which effective mass is desired.

Then one must calculate the pseudo modal participation factors. The first pseudo modal participation factor is for the rigid body mode and is calculated as

$$pmpf(1) = m_{TA}\Psi_B^1 \tag{3}$$

where m_{TA} is the mass of the test article and Ψ_B^1 is the mass normalized mode shape of the rigid body mode on the base (test fixture) in the direction of interest. The pseudo modal participation factor for each elastic mode is calculated as

$$pmpf(k) = -M_B\Psi_B^k \tag{4}$$

where M_B is the mass of the base (test fixture) and is the mode shape of the particular elastic mode on the base (test fixture). The estimate of the modal participation factors are calculated from

$$P_k = \left[pmpf(1) \quad pmpf(2) \quad \ldots \quad pmpf(n)\right]\bar{\mathbf{a}}_k \tag{5}$$

where $\bar{\mathbf{a}}_k$ is the kth column of $\mathbf{L\Gamma}$.

7) Modal Test of Fixture with Truth Plate

To capture the elastic fixture modes, the bare fixture without test articles was suspended by a small bungee cord and impacted with a PCB Model 086C01 with white plastic tip. The sensitivity of the hammer was confirmed by impacting a suspended 4.5 kg mass with a calibrated accelerometer, and it reproduced the analytical mass line within two percent. An elastic mode at about 5,464 Hz was extracted for the bare fixture which looked like a standard first plate twisting mode. Then the truth plate was attached by two screws to the fixture and the hardware shown in the right side of Figure 1 was suspended with a small bungee cord. Two sets of FRFs were gathered for accelerometers mounted on the fixture. In one set the impact was at the center of the fixture, and in the other the impact was at one corner (not one of the corners with a mounting post). Accelerometers were attached to the fixture as shown in **Error! Reference source not found.**Figure 3. Accelerometers

measured in the Y and Z directions for node 101, the XYZ directions for node 102, the X and Y directions for node 103 and only the Y direction for nodes 104 and 105. Mode shapes for both FRF data sets were extracted using a Sandia in-house algorithm SMAC[9].

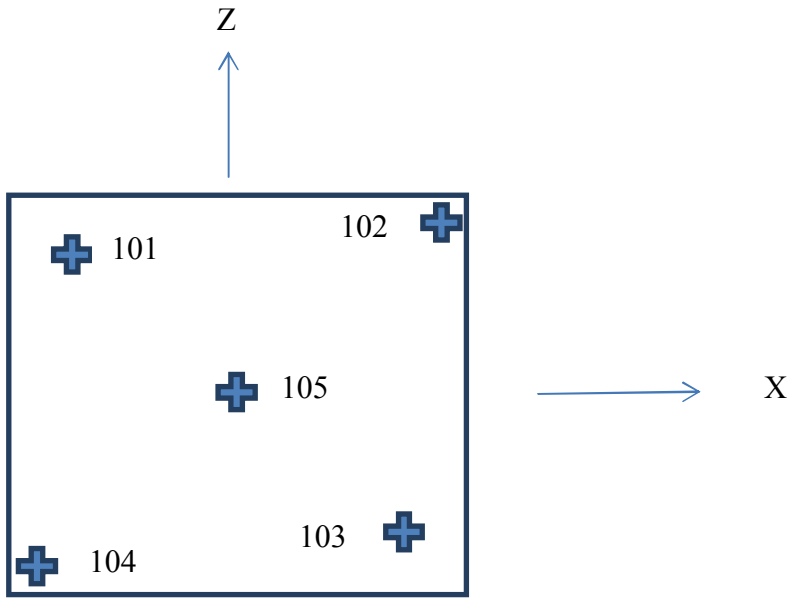

Figure 3 - Accelerometer Layout on the Aluminum Fixture

The imaginary portion of the driving point FRF for each data set is shown in Figure 4 and Figure 5. The actual data are in blue and the FRF synthesized from the modal parameters are in green. Three distinct modes and one weak one were extracted from the center of plate impacts and seven were extracted from the corner of the plate data.

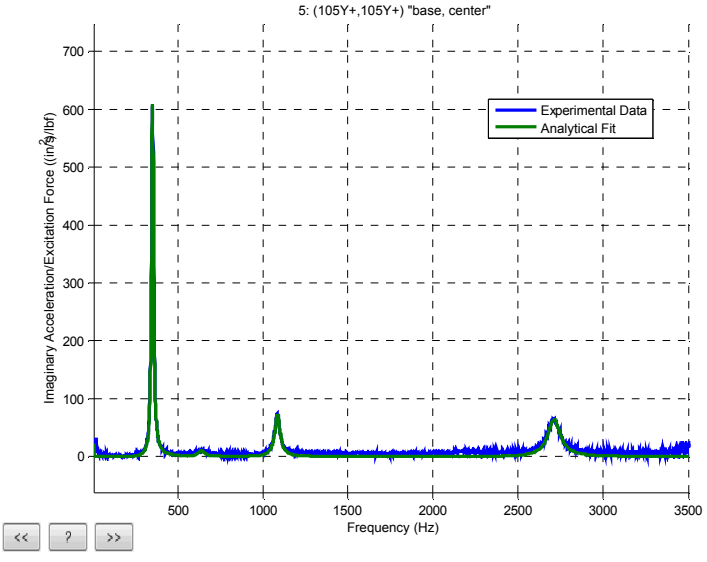

Figure 4 - Drive Point FRF and Synthesis for Center of Plate

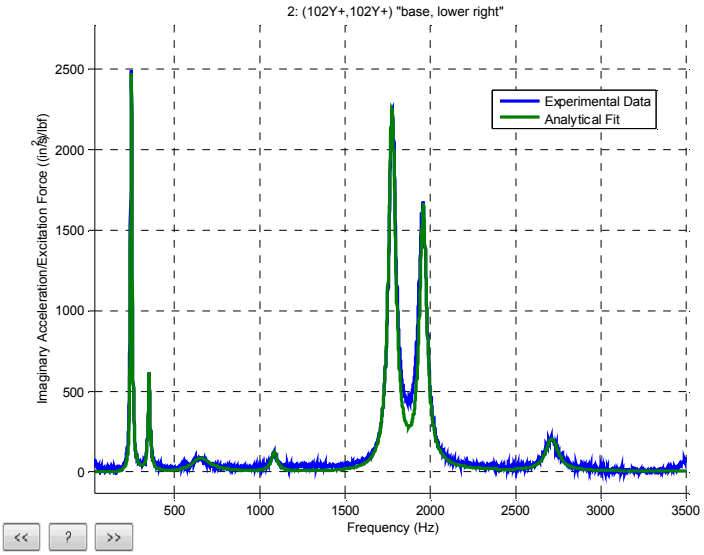

Figure 5 - Drive Point FRF and Synthesis for Corner of Plate

The center plate impact tends to excite modes that have effective mass in the direction of impact while the corner plate impact excites those modes plus anti-symmetric modes that may not have much effective mass in the translation direction. In addition to the elastic modes extracted from test, the rigid body mode shapes were analytically calculated and added to these data sets for processing to extract effective mass in the Y direction.

8) Finite Element Model Truth Calculations

The truth calculations for the effective mass comparisons came from finite element model simulations utilizing NX NASTRAN were performed by ATA Engineering. The fixture was modeled, and its first mode is shown in Figure 6. The nylon plate was modeled as isotropic and its modulus was tuned to match the first free mode of the nylon plate by itself at 646 Hz. Its first mode is shown in Figure 7. Then the nylon plate was mounted to the fixture by equivalencing the nodes at the post. This result produced a natural frequency that was slightly higher than what was seen in the modal test of the fixture and nylon plate. The boundary condition was adjusted to include some springs to better match the first test mode. Then the modes of the nylon plate were calculated with the fixed and the springs fixed to ground to give bounds on the effective mass of each mode of the plate. This is why there is a range of effective mass shown in the previous tables.

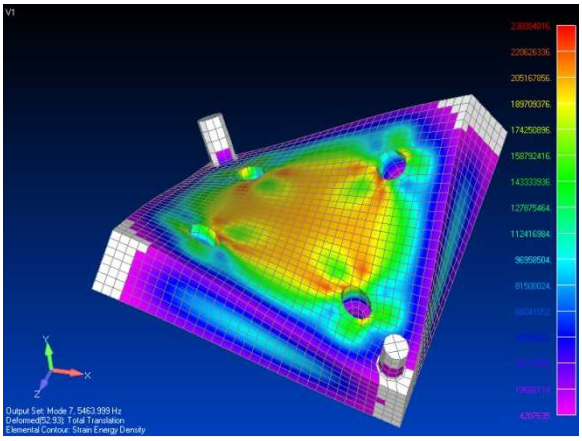

Figure 6 – FE Model of First Fixture Elastic Mode

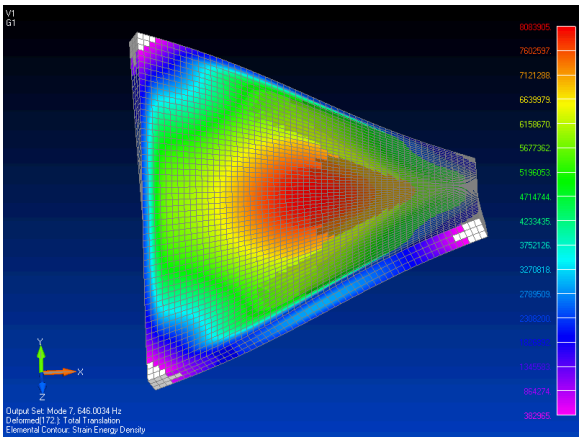

Figure 7 - First Free Elastic Mode of Nylon Plate

The mode shapes for the nylon plate fixed at the two posts are given in Figure 8. The fixed frequencies for the equivalence and spring boundary conditions and the constrained test data are shown in Table 1. Note that modes 4, 5 and 9 would not be excited well by impacting at the center or the unsupported corner. They would be excited by impacting at a supported corner, which we did not impact. There is pretty good agreement for the first couple of fixed frequencies between the FE spring model and the test data. At higher frequencies there are greater discrepancies, and the test results should be more accurate for the higher modes, even with the constraining mathematics because the fixed base modes are only very slightly different than the free modes of the nylon plate attached to the fixture. So there may be a bit of error in the FE model estimates of effective mass which we are considering "truth".

Table 1 - Fixed Frequencies for Modes of Nylon Plate

Mode No.	Test Frequency (Hz)	Equivalenced FE Frequency	Spring FE Frequency
1	238	264	240
2	339	357	344
3	1081	1012	1000
4	-	1179	1110
5	-	1235	1182
6	1683	1836	1775
7	1920	2244	2070
8	2705	2654	2590
9	-	2733	2619

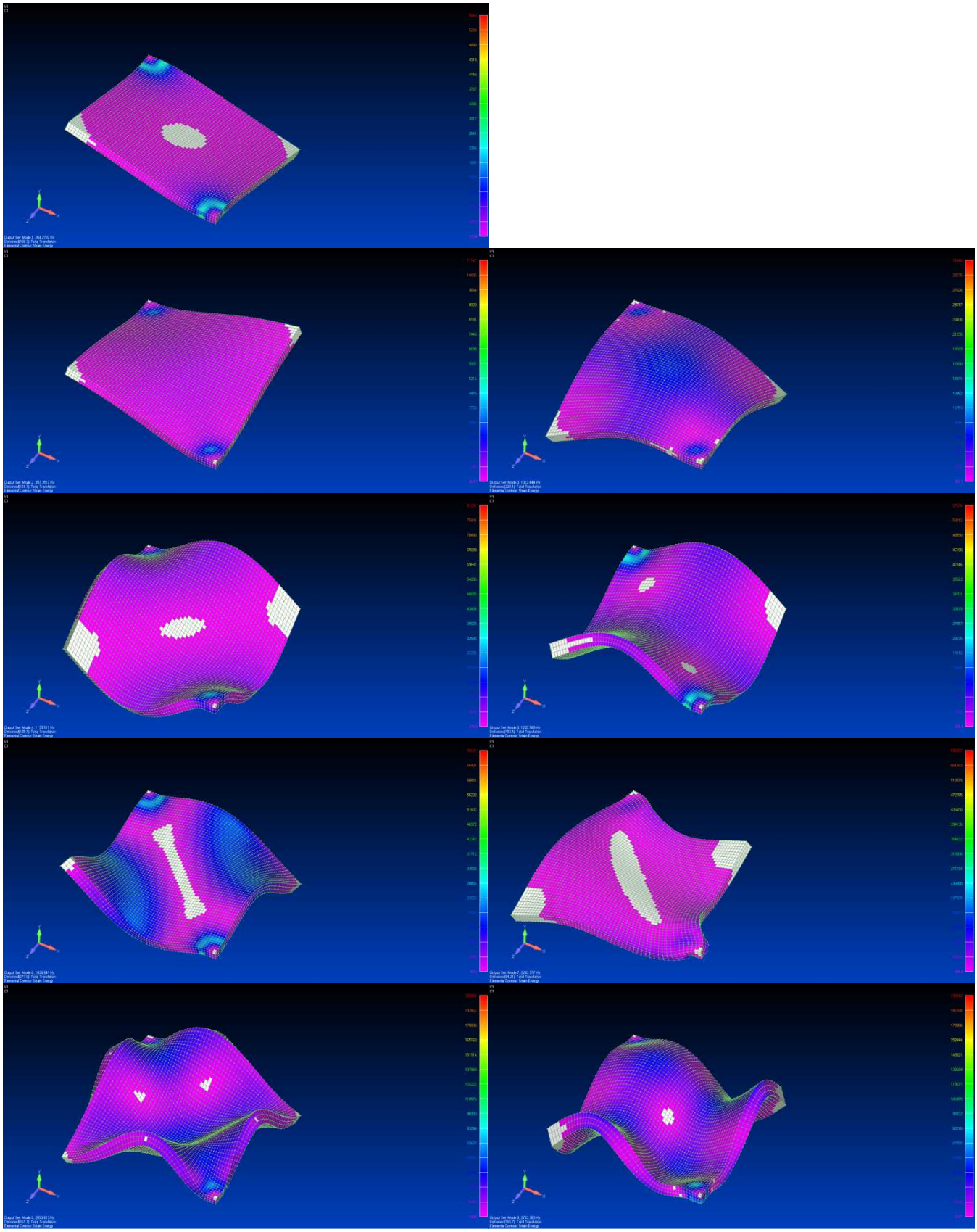

Figure 8 - Mode Shapes of Nylon Plate Fixed at Nearest and Farthest Corner

9) Experimental Effective Mass Extractions

The effective mass extraction procedure was applied to both sets of data to obtain the Y direction effective mass. The best results for effective mass came from the center plate impact and are given in Table 2. These results are normalized to the total mass of the test article. The difference between the test result and the truth FE result is expressed as the percentage of the TOTAL mass of the test article.

Table 2- Normalized Test Effective Mass from Center Plate Impact Compared to FE Model

Test Frequency (Hz)	Effective Mass from Test	Effective Mass from FE Model	Difference as % of Total Mass of Test Article
339.4	0.815	0.816-0.831	-0.1 to -1.6
638.6	0.018	-	-
1081.4	0.069	0.058-0.062	-1.1 to -0.7
2705	0.040	0.0041-0.0043	-0.01 to -0.03

The results for normalized effective mass from the corner plate impact are given in Table 3.

Table 3- Normalized Test Effective Mass from Corner Impact Compared to FE Model

Test Frequency (Hz)	Effective Mass from Test	Effective Mass from FE Model	Difference as % of Total Mass of Test Article
238.2	.0000	.0000	0
340.1	0.788	0.816-0.831	-2.8 to -4.3
650.2	0.016	-	-
1082.6	0.057	0.058-0.062	-0.1 to -0.5
1683	.0000	.0000	0
1920	.0000	.0000	0
2712	0.028	0.0041-0.0043	2.4

Table 3 results provide some additional interesting information. There are three modes that have zero normalized effective mass out to four decimal places. The fact that these zero effective mass modes are predicted with zero effective mass is encouraging. The highest effective mass has more error than from the center plate result. In pondering why this might be, it was noticed that the impact mark for the 102 node was slightly out of line from the 102Y accelerometer. So this slight misalignment could be affecting the accuracy. It should be noted that accurate dimensions, mass properties and accelerometer placements and hammer impact locations are required to get accurate rigid body mode shapes and FRFs.

10) Test Anomaly

In Tables 1 and 2 one may notice a test mode with a small effective mass that does not correspond to any FE mode. This rogue mode was studied further to determine its cause. The modal damping was nearly 10 percent for this mode around 640 Hz, and it was extracted from both data sets. Eventually the cause was discovered. This is a false mode. This can be explained by investigating the FRF, and the autospectra of the drive point accel and the force which are shown in Figure 9. Notice that in the FRF there are four resonances, but in the accelerometer autospectrum only three resonances. In the hammer force autospectrum one can see an anomaly (circled in red) which is not uncommon in certain hammers. This is a pollution of the autospectrum due to the first bending mode of the hammer. After impact the hammer vibrates which causes this dynamic effect. This effect is not sensed by the accelerometer because the impact is over. This produces a false mode in the data.

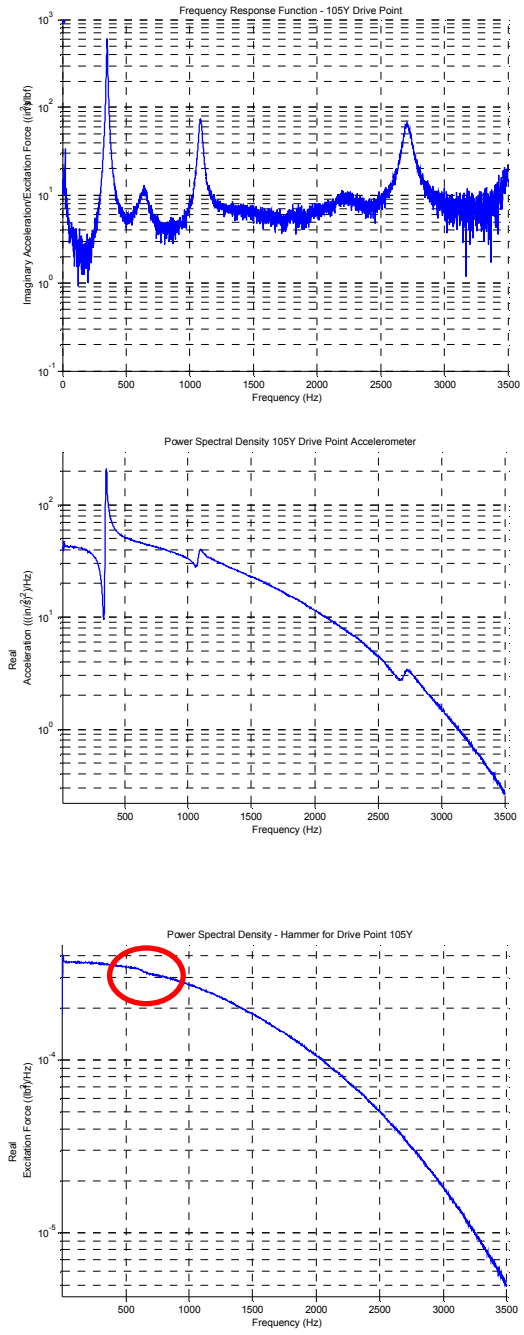

Figure 9 - Cause of Rogue Mode - FRF/Accel Autospectrum/Hammer Autospectrum

11) Effective Mass of Circuit Board

The circuit board on the left side of Figure 1 was tested in the same manner as the nylon plate with the center plate hammer impact. Normalized effective mass extractions are shown in Table 4. The uncertainty is assumed to be on the order of 0.02 from the previous work.

Table 4 - Normalized Test Effective Mass for Circuit Board

Test Frequency (Hz)	Effective Mass from Test
134	0.170
181	0.640
654	0.057
725	0.012
1065	0.016
1174	0.003
1416	0.009
1650	0.008
2031	0.001
2174	0.004
2283	0.005

12) Conclusions

Effective mass was calculated from the center impact reference for three modes to within two percent of the total mass of the test article, when compared with a FE truth model. A corner impact reference resulted in effective mass for three additional modes as zero out to four decimal places, which agreed with the truth model. The corner impact reference data produced effective mass within five percent of the total mass of the test article when compared with the truth model. It was found that the corner impact setup had a slight misalignment of the impact location with the drive point accelerometer which could have impaired its results slightly, since that would affect the mode shape and modal mass extraction. Accurate rigid body mode shapes as well as extracted elastic mode shapes are required for the data processing to extract effective mass from experiment. A false mode was discovered in the truth test, which was due to the dynamics of the hammer, which appeared to have a normalized effective mass of nearly 0.02. The effective mass extraction process appears to be fairly robust for the truth test geometry and setup since the FRFs seem to exhibit linear behavior.

13) Acknowledgments

The authors thank David Najera and Paul Blelloch of ATA Engineering for providing the FE analyses and figures.

References

1 Savoie, Troy and Babuska, Vit, "Fatigue Testing of a Circuit Board in a Designed Experiment", *Proceedings of the 32nd International Modal Analysis Conference*, Orlando, FL, February 2014, paper number 296.

2 Mayes, Randy L., Schoenherr, Tyler F., Blecke, Jill and Rohe, Daniel P., "Efficient Method of Measuring Effective Mass of a System", *Proceedings of the 31st International Modal Analysis Conference*, Garden Grove, California, February 2013, paper number 194.

3 Wada, Ben K., Bamford, Robert, and Garba, John A., "Equivalent Spring-Mass System: A Physical Interpretation", *The Shock and Vibration Bulletin*, US Naval Station – Key West, FL, January 1972, pp 215-224.

4 Mayes, Randy L. and Bridgers, L. Daniel, "Extracting Fixed Base Modal Models from Vibration Tests on Flexible Tables", *Proceedings of the 27th International Modal Analysis Conference*, Orlando, FL, February 2009, paper 67.

5 Allen, Matthew S., Gindlin, Harrison M. and Mayes, Randall L., "Experimental modal substructuring to estimate fixed-base modes from tests on a flexible fixture", *Journal of Sound and Vibration*, Vol 330 (2011), pp. 4413-4428.

6 Mayes, Randy L. and Allen, Matthew S., "Converting a Driven Base Vibration Test to a Fixed Base Modal Analysis", *Proceedings of the 29th International Modal Analysis Conference*, Jacksonville, Florida, 2011, paper 36.

7 Mayes, Randy L., "Refinements on Estimating Fixed Base Modes on a Slip Table", *Proceedings of the 30th International Modal Analysis Conference*, paper 162, February 2012.

8 De Klerk, D., Rixen, D.J., and Voormeeren, "General framework for dynamic substructuring: History, review, and classification of techniques", *AIAA Journal*, Vol. 46, no. 5 (2008), pp. 1169-1181.

9 Hensley, Daniel P., and Mayes, Randall L., "Extending SMAC to Multiple References", *Proceedings of the 24th International Modal Analysis Conference,* pp.220-230, February 2006.
10 http:/www.ce.memphis.edu/7119/fema_notes.htm, Topic 4 Notes.